

Barium Bismuthate Nanoribbons with Good Electrochemical Detection Performance for Pb(II)

Mao-Ting Ding¹, Xian-Zhang Ling^{1,2,*}, F. F. Lin¹, L. Pei^{1,*}, C. G. Fan¹

¹ School of Civil Engineering, Harbin Institute of Technology, Heilongjiang, Harbin 150090, P. R. China

² School of Civil Engineering, Qingdao Technological University, Shandong, Qingdao 266520, P. R. China

*E-mail: xianzhang_ling@263.net, lzpei1977@163.com

Received: 4 April 2017 / Accepted: 10 August 2017 / Published: 12 September 2017

A facile hydrothermal process was used for the synthesis of barium bismuthate nanoribbons. The nanoribbons were applied as the sensing materials for sensitive detection of Pb(II). The micromorphology and structure of the prepared products were analyzed by scanning electron microscopy (SEM) and X-ray diffraction (XRD), respectively. The suspension with barium bismuthate nanoribbons was cast on the surface of a glassy carbon electrode (GCE). The barium bismuthate nanoribbons modified GCE was used for the detection of Pb(II) using square wave anodic stripping voltammetry (SWASV) technique. The results show that the fabricated GCE exhibited a linear range of 0.001-2 mM with the limit of detection (LOD) of 0.13 μ M. The barium bismuthate nanoribbons modified GCE has a promising potential in practical application for the detection of real samples with water and soil.

Keywords: Barium bismuthate nanoribbons, Glassy carbon electrode, Scanning electron microscopy, Electrochemical detection, Pb(II).

1. INTRODUCTION

Heavy metal ions, such as Pb (II) and Cd (II) are usually accumulated in soil and water, and can not be bio-degraded. Heavy metal ions are considered as the serious source to pollute the environment and cause many physiological and healthy disease owing to their toxicity [1-4]. Therefore, it is of great significance for the detection of toxic heavy metal ions in the soil and water so as to protect the environment and human health. To date, various methods have been proposed for the analysis of heavy metal ions, such as optical methods [5], mass spectrometric method [6] and

electrochemical method [7,8]. Among these methods, optical and mass spectrometric method can simultaneously detect various heavy metal ions with high selectivity and sensitivity. However, these methods require expensive instruments and complicated detection process which is not suitable for in-situ analysis of heavy metal ions. Great interest has been devoted to electrochemical method owing to high sensitivity, low cost, short measurement time, adaptability for in-situ measurement and portability [9,10]. Solid electrodes that modified by different nanoscale materials have been developed for the detection of heavy metal ions [11-13]. However, the electrochemical detection ability still need to be enhanced by exploring novel nanoscale electrode materials.

Bismuth-based materials show good electrochemical performance and have been recognized as the effective electrode materials for the analysis of heavy metal ions owing to their unique physical, chemical and electronic properties [14-17]. Barium bismuthate nanoscale materials belong to important bismuth-based materials. Compared with bulk barium bismuthate, barium bismuthate nanoscale materials may possess higher catalytic activity and electrochemical performance due to large specific surface area, extensive active sites, high surface free energy and enhanced electronic property [18]. These stimulate us to research the barium bismuthate nanoscale materials for the detection of heavy metal ions in soil and water. However, to date, only bulk barium bismuthate was prepared by high temperature solid method [19-21]. Barium bismuthate nanoscale materials were not reported.

Various nanoscale materials can be effectively synthesized by the facile hydrothermal process [22-24]. In this work, barium bismuthate nanoribbons have been synthesized by a facile hydrothermal approach using hexadecyl trimethyl ammonium bromide (CTAB) as the surfactant. The micromorphology and structure of the products were analyzed by X-ray diffraction (XRD) and scanning electron microscopy (SEM), respectively. The glassy carbon electrode (GCE) was modified by barium bismuthate nanoribbons using the mechanical attachment method. The barium bismuthate nanoribbons modified GCE showed good electrochemical performance for the detection of Pb (II) with wide detection range, low limit of detection (LOD), high sensitivity and good stability. The results show that the barium bismuthate nanoribbons modified GCE is a promising candidate for the electrochemical detection of Pb (II).

2. EXPERIMENTAL PROCEDURE

Sodium bismuthate and barium acetate were purchased from Aladdin Reagent Co., Ltd. of P. R. China. CTAB was purchased from Sinopharm Chemical Reagent Co., Ltd. of P. R. China. All reagents were AR grade. 0.1 M KCl buffer solution was prepared using de-ionized water and potassium chloride. Barium bismuthate nanoribbons were synthesized in the following procedure by a simple surfactant-assisted hydrothermal route. Barium acetate and sodium bismuthate with the molar ratio of 1:1, and 5wt.% CTAB were mixed with 60 mL de-ionized water at room temperature under stirring. Then the mixtures were sonicated at room temperature for 30 min. The mixtures were transferred and sealed into a 100 mL Teflon-lined stainless autoclave. The autoclave was heated at 180 °C in an oven for 24 h. The resulting products were centrifuged and washed with de-ionized water and alcohol for several times. Finally, barium bismuthate nanoribbons were obtained by drying at 60 °C in air.

SEM image of the sample was observed using a nova FEI 430 (FEI, Tokyo, Japan) scanning electron microscopy operated at 15 kV accelerating voltage. To analyze the phase of the products, XRD pattern was obtained using a Bruker AXS D8 X-ray diffractometer in 2θ range of 20° to 60° with $\text{Cu K}\alpha$ radiation.

Barium bismuthate nanoribbons were dispersed into N, N-dimethylformamide (DMF) solution to form a suspension (1.0 mg mL^{-1}) under stirring for 1 h. Before the modification, bare GCE with the diameter of 3 mm was polished carefully using $0.05 \mu\text{m}$ alumina slurry, rinsed with de-ionized water and alcohol for several times. Then the electrode was dried to form a mirror-like surface. $10 \mu\text{L}$ solution with the barium bismuthate nanoribbons was pipetted onto bare GCE. The solvent was evaporated using an infrared lamp to obtain barium bismuthate nanoribbons modified GCE.

Electrochemical experiments were performed using a CHI620E computer-controlled potentiostat (Shanghai Chenhua Instrument Co., P. R. China). A barium bismuthate nanoribbons modified GCE was used as a working electrode, a platinum electrode and saturated Ag/AgCl electrode acted as the counter electrode and reference electrode, respectively. Electrochemical impedance spectroscopy (EIS) was measured in $1 \text{ mM K}_3\text{Fe}(\text{CN})_6$ solution containing 0.1 M KCl . Square wave anodic stripping voltammetry (SWASV) was applied for the analysis of Pb(II) with a deposition potential of -1.0 V for 120 s by the reduction of Pb(II). The anodic stripping of the electro-deposited metal was carried out in the potential range of -0.5 V to 1.0 V at the following parameters: Frequency, 15 Hz, increment potential, 4 mV, amplitude, 25 mV.

3. RESULTS AND DISCUSSION

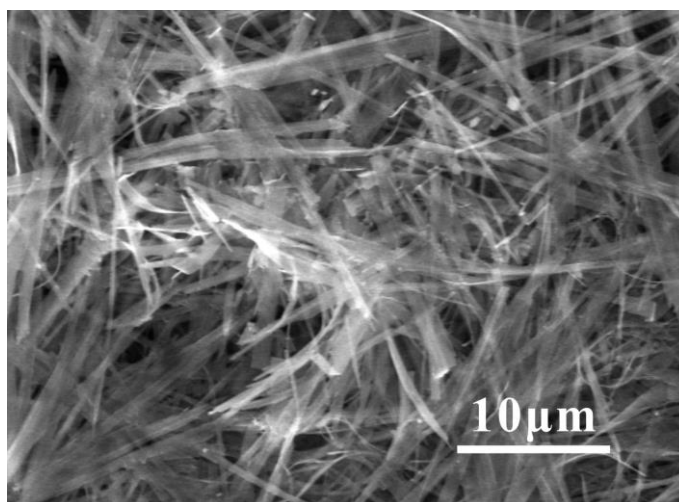


Figure 1. SEM image of the sample synthesized from 180°C for 24 h using 5wt.% CTAB.

Figure 1 shows the SEM morphology of the products obtained from 180°C for 24 h. It is observed that uniform nanoscale ribbon-shaped morphology with smooth surface is formed in the products. The length of the nanoribbons is several dozens of micrometers, the average width and

thickness of the nanoribbons are about 500 nm and 50 nm, respectively. The nanoribbon-shaped morphology is similar to that obtained from similar surfactant-assisted hydrothermal route [25-27].

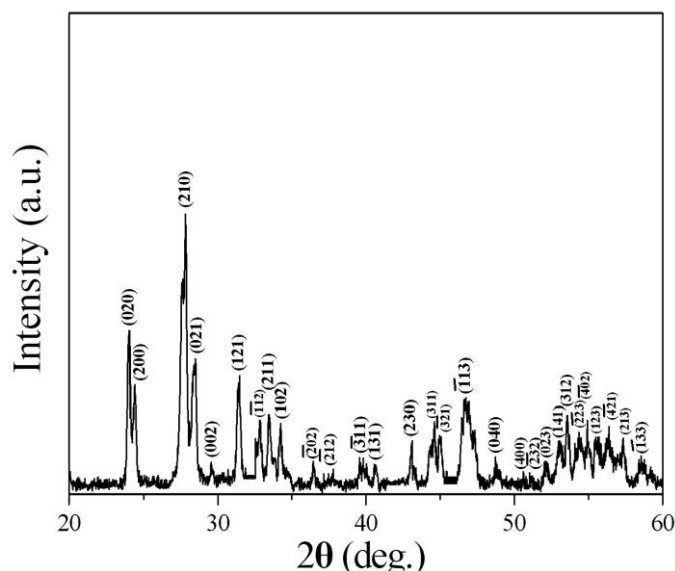


Figure 2. XRD pattern of the sample synthesized from 180 °C for 24 h using 5wt.% CTAB.

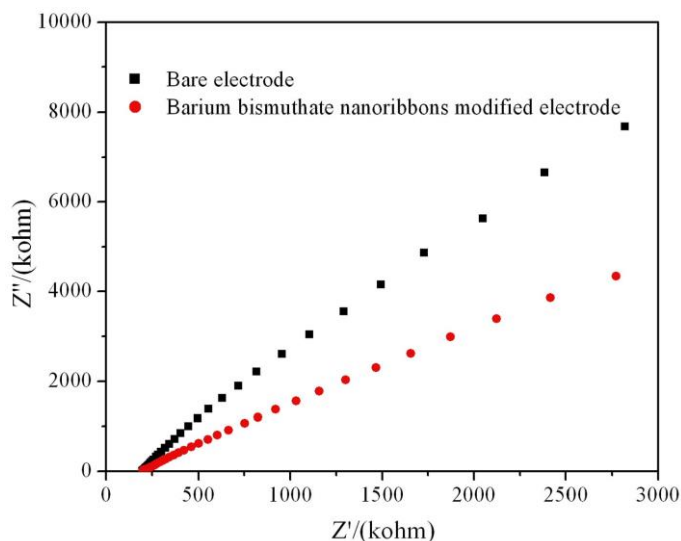


Figure 3. EIS of bare GCE and barium bismuthate nanoribbons modified GCE. $K_3Fe(CN)_6$, 1 mM, KCl, 0.1 M.

The crystal structure of the products was analyzed by powder XRD. As shown in figure 2, the nanoribbons exhibit the diffraction peaks of monoclinic $BaBiO_{2.5}$ phase (JCPDS card No. 50-0854). Besides monoclinic $BaBiO_{2.5}$ phase, no other phases are indexed. Combining analysis of the SEM image and XRD pattern, it is confirmed that the products are composed of barium bismuthate nanoribbons. It is noticed that the barium bismuthate nanoribbons are obtained by the CTAB-assisted hydrothermal process. Similar to the nanoribbons with different compositions synthesized by other

groups [28,29], CTAB molecules act as the structure-directing agent that inducing the formation of the barium bismuthate nanoribbons.

EIS was applied to characterize the interface performance of the barium bismuthate nanoribbons modified GCE. Figure 3 shows the EIS of the bare GCE and barium bismuthate nanoribbons modified GCE. Generally, in the Nyquist plot, the electron transfer ability between the electrode and buffer solution depends on the diameter of the semicircle portion of Nyquist circle. After the modification of the barium bismuthate nanoribbons on the GCE, the diameter of the semicircle is smaller than that of the bare GCE. The result suggests that the barium bismuthate nanoribbons modified GCE has better electron transfer ability than that of the bare GCE.

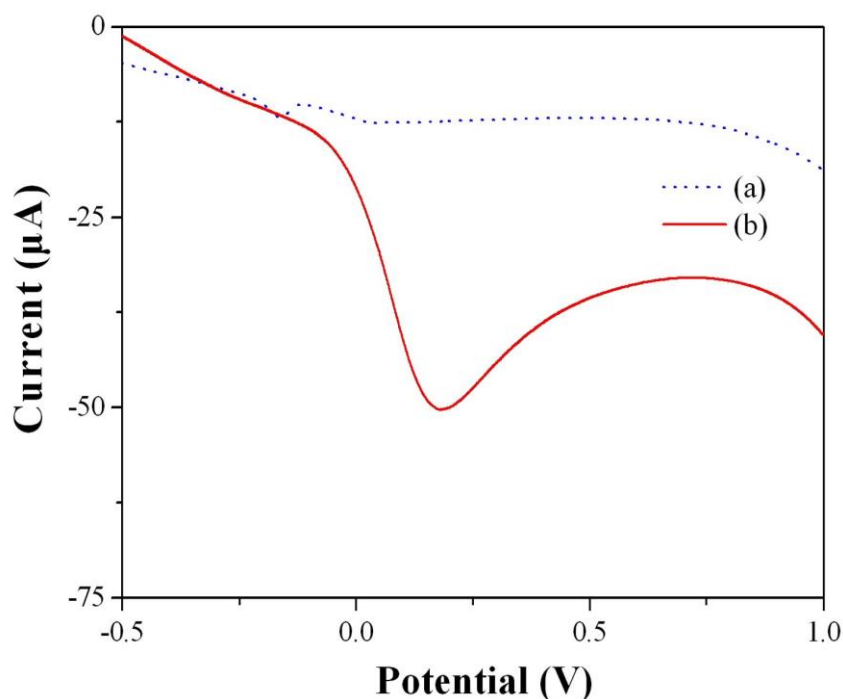


Figure 4. Square wave anodic stripping voltammetry (SWASV) response for the analysis of 2 mM Pb(II) at bare GCE (a) and barium bismuthate nanoribbons modified GCE (b) in 0.1 M KCl solution. Supporting electrolyte, 0.1 M KCl buffer solution (pH=7.0).

Figure 4 shows the SWASV analytical performance of the bare GCE and barium bismuthate nanoribbons modified GCE. The analysis process was performed at -1.0 V for 120 s in the solution containing 2 mM Pb(II) in 0.1 M KCl (pH=7.0). Very weak peak at the bare GCE is observed (Figure 4a) which may originate from poor absorbability of the bare GCE toward Pb(II) [8]. A higher and sharper peak current for Pb(II) at +0.18 V is obtained at the barium bismuthate nanoribbons modified GCE (Figure 4b). The result shows that the barium bismuthate nanoribbons modified GCE has better response toward Pb(II) than that at the bare GCE. Obviously, ranging from -0.5 V to +1.0 V, the high and sharp stripping current shows that the barium bismuthate nanoribbons are suitable for the detection of Pb(II).

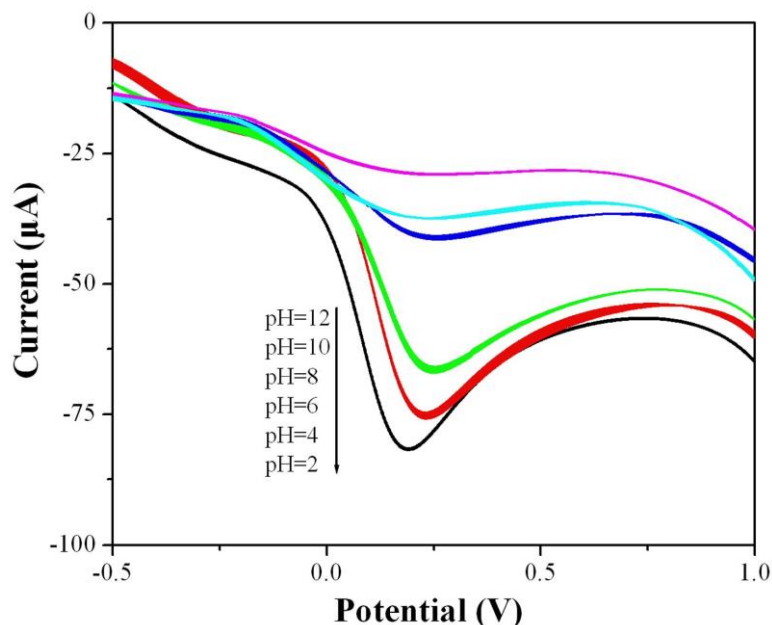


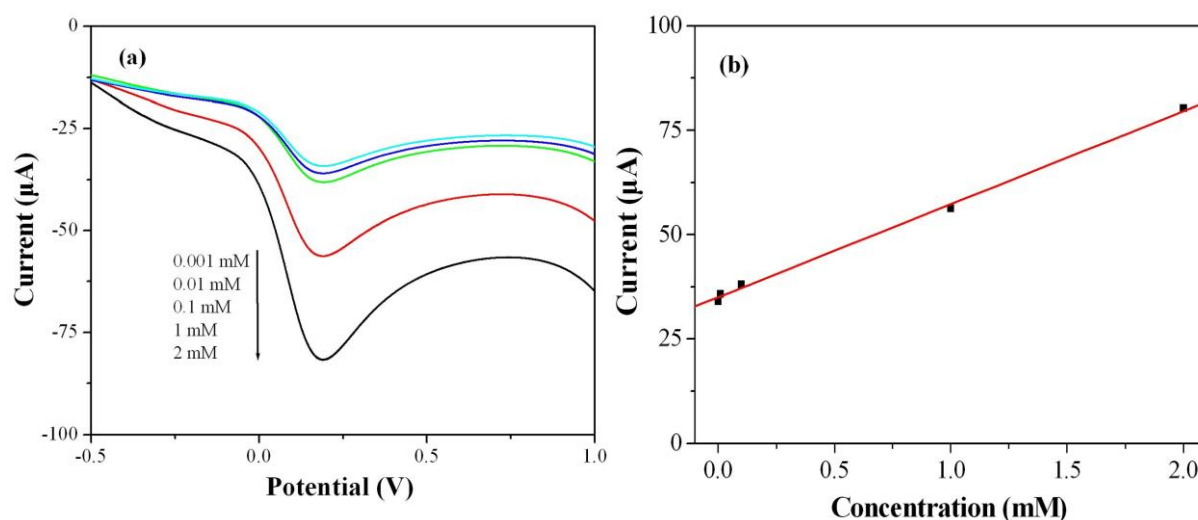
Figure 5. SWASV response of 2 mM Pb(II) at the barium bismuthate nanoribbons modified GCE in the KCl solution with different pH values.

pH value of the buffer solution plays an important role in the voltammetric response for the detection of heavy metal ions at the modified GCE [1,2,4]. To promote the Pb(II) detection ability of the barium bismuthate nanoribbons modified GCE, the pH value of the buffer solution was optimized. Figure 5 shows the SWASV responses of the barium bismuthate nanoribbons modified GCE for the analysis of 2 mM Pb(II) in KCl buffer solution in the pH value ranging from 12 to 2. It is showed that the peak current increases obviously with the pH value changing from 12 to 2. The peak current reaches a maximum at the pH value of 2. Therefore, 0.1 M KCl buffer solution (pH=2) is selected for the stripping measurements.

The LOD was determined using the barium bismuthate nanoribbons modified GCE. Figure 6a shows the SWASV response of the barium bismuthate nanoribbons modified GCE for the analysis of Pb(II) with different concentrations. The stripping peak current increases proportionally to the Pb(II) concentration. The corresponding calibration curve shows linear range from 0.001 to 2 mM (Figure 6b). The linearization equation for the detection of Pb(II) is $I/\mu\text{A}=34.842+22.579c/\text{mM}$. The correlation coefficient is 0.9985. The LOD is calculated to be 0.13 μM for Pb(II) according to 3σ method. Table 1 lists the comparison of the analysis parameters for Pb(II) using different electrodes. Comparing with the analytical parameters for Pb(II), such as LOD and linear range [2, 8, 32-39], the barium bismuthate nanoribbons modified GCE shows a wide linear range and comparable LOD. The results show that the barium bismuthate nanoribbons modified GCE has a good electrochemical performance for the detection of Pb(II).

Table 1. Comparison of the analysis parameters for Pb(II) using different electrodes.

Electrodes	Linear range (μM)	Detection limit (μM)	Ref
Amidogen functional carbon microsphere modified GCE	0.6-1.8	0.383	2
AlOOH-reduced graphene oxide nanocomposites modified GCE	0.3-1.1	7.6×10^{-5}	8
Antimony film electrode	0.3-1.0	3.66×10^{-3}	32
Fe_3O_4 nanocrystals modified GCE	0.1-1.0	0.12	33
Graphene nanodots-encaged porous gold electrode	0.006-2.5	6×10^{-3}	34
Bismuth oxide electrode	0.097-1.4	0.039	35
Magnesium silicate hollow nanospheres modified GCE	0.2-1.0	2.47×10^{-4}	36
Bismuth nanoribbons modified screen printed carbon electrode	0.12-0.61	1.27×10^{-3}	37
Polymer carbon paste electrode	9.76-610	2.44	38
Reduced graphene oxide modified bismuth electrode	0.012-1.22	4.88×10^{-3}	39
Barium bismuthate nanoribbons modified GCE	0.001-2	0.13	This work

**Figure 6.** (a) SWASV response of Pb(II) with different concentrations at the barium bismuthate nanoribbons modified GCE. Electrolyte, 0.1 M KCl solution with the pH value of 2.0. (b) The linear calibration curve of the peak current against Pb(II) concentration.

The repeatability of the barium bismuthate nanoribbons was performed in parallel experiments for 20 times. Figure 7 shows the SWASV responses of 2 mM Pb(II) at the barium bismuthate nanoribbons modified GCE after 20 successive scans. The stripping current on the barium bismuthate nanoribbons modified GCE is steady. The relative standard deviation is 1.59%. The result shows that

the barium bismuthate nanoribbons modified GCE has good stability for the repeated detection of Pb(II) and is suitable for the analysis of real samples.

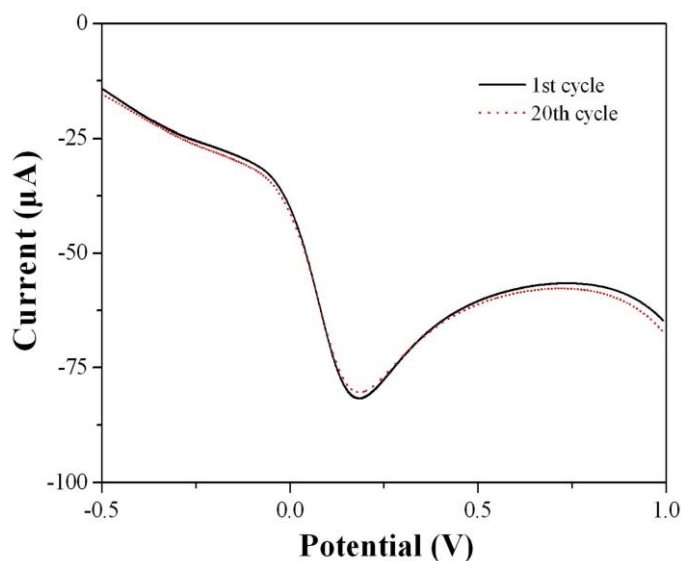


Figure 7. SWASV response of 2 mM Pb(II) at the barium bismuthate nanoribbons modified GCE for the 1st and 20th time. Electrolyte, 0.1 M KCl solution with the pH value of 2.0.

Pb(II) usually exists in the soil and water. The validity of the proposed detection method using barium bismuthate nanoribbons modified GCE is investigated by detecting Pb(II) in real sample with tap water and soil. Soil and tap water with the mass ratio of 1:19 were mixed forming the real sample. The known amount of Pb(II) was added. The recovery of Pb(II) was determined by standard addition and the results are shown in Table 2. The recovery is varied from 97.8% to 103.4%. The result suggests that the barium bismuthate nanoribbons have potential practical application in the environments with water and soil.

Table 2. Detection of Pb(II) using barium bismuthate nanoribbons modified GCE in tap water and soil.

Sample (Tap water with soil)	Amount added/ μM	Amount found/ μM (average of five times)	Recovery/%
1	5	4.89 ± 0.12	97.8
2	20	19.84 ± 0.19	99.2
3	40	41.36 ± 0.28	103.4

4. CONCLUSIONS

In summary, barium bismuthate nanoribbons were synthesized using a simple CTAB-assisted hydrothermal process. The nanoribbons with monoclinic BaBiO_{2.5} phase have the length, width and

thickness of about several dozens of micrometers, 500 nm and 50 nm, respectively. The GCE is modified with barium bismuthate nanoribbons. SWASV responses of Pb(II) at the modified GCE show that the barium bismuthate nanoribbons are suitable for the analysis of Pb(II). The peak current increases obviously with the pH value changing from 12 to 2. The LOD is 0.13 μM . The barium bismuthate nanoribbons have the promising potential for the practical application in real sample with water and soil.

ACKNOWLEDGEMENTS

The research is supported by the Major Scientific Instrument Development Project of National Natural Science Foundation of China (No. 41627801).

References

1. L. Cui, J. Wu and H. X. Ju, *Biosens. Bioelectr.*, 63 (2015) 276.
2. Y. F. Sun, L. J. Zhao, T. J. Jiang, S. S. Li, M. Yang and X. J. Huang, *J. Electroanal. Chem.*, 760 (2016) 143.
3. H. Serencam, D. Ozdes, C. Duran and M. Tufekci, *Environ. Monit Assesss*, 185 (2013) 6003.
4. X. L. Yu, S. R. Tong, M. F. Ge, L. Y. Wu, J. C. Zuo, C. Y. Cao and W. G. Song, *J. Environ. Sci.-China*, 25 (2013) 933.
5. A. N. Uglov, A. Bessmertnykh-Lemeune, R. Guilard, A. D. Averin and I. P. Beletskaya, *Rus. Chem. Rev.*, 83 (2014) 196.
6. P. Ugo, S. Zampieri, L. M. Moretto and D. Paolucci, *Anal. Chim. Acta*, 434 (2001) 291.
7. X. Xuan, M. D. F. Hossain and J. Y. Park, *J. Nanosci. Nanotechnol.*, 16 (2016) 11421.
8. C. Gao, X. Y. Yu, R. X. Xu, J. H. Liu and X. J. Huang, *ACS Appl. Mater. Interfaces*, 4 (2012) 4672.
9. V. K. Gupta, H. Mahmoody, F. Karimi, S. Agarwal and M. Abbasghorbani, *Int. J. Electrochem. Sci.*, 12 (2017) 248.
10. P. ReddyPrasad, A. E. Ofamaja, C. N. Reddy and E. B. Naidoo, *Int. J. Electrochem. Sci.*, 11 (2016) 65.
11. M. B. Gumpu, S. Sethuraman, U. M. Krishnan and J. B. B. Rayappan, *Sens. Actuat. B: Chem.*, 216 (2015) 515.
12. D. Bagal-Kestwal, M. S. Karve, B. Kakade and V. K. Pillai, *Biosens. Bioelectr.*, 24 (2008) 657.
13. S. Mohan, F. Okumu, O. Oluwafemi, M. Matoetoe and O. Arotiba, *Int. J. Electrochem. Sci.*, 11 (2016) 745.
14. L. Cui, J. Wu and H. X. Ju, *Chem. Eur. J.*, 21 (2015) 11525.
15. S. Arlt, J. Harloff, A. Schulz, A. Stoffers and A. Villinger, *Inorg. Chem.*, 55 (2016) 12321.
16. Y. Z. Sun, M. Yang, J. Q. Pan, P. Y. Wang, W. Li and P. Y. Wan, *Electrochim. Acta*, 197 (2016) 68.
17. N. Serrano, A. Alberich, J. M. Diaz-Cruz, C. Arino and M. Esteban, *TrAC Trends Anal. Chem.*, 46 (2013) 15.
18. K. E. Toghill and R. G. Compton, *Electroanalysis*, 22 (2010) 1947.
19. Y. Yacoby, S. M. Heald and E. A. Stern, *Solid State Commun.*, 101 (1997) 801.
20. B. Rasche, W. V. Broek and M. Ruck, *Chem. Mater.*, 28 (2016) 665.
21. C. Chaillout and J. P. Remeika, *Solid State Commun.*, 56 (1985) 833.
22. L. W. Lin, Y. H. Tang, C. S. Chen and H. F. Xu, *CrystEngComm*, 12 (2010) 2975.
23. L. W. Lin, Y. H. Tang and C. S. Chen, *Nanotechnology*, 20 (2009) 175601.
24. L. Z. Pei, N. Lin, T. Wei, H. D. Liu and H. Y. Yu, *J. Mater. Chem. A*, 3 (2015) 2690.

25. M. S. Bakshi, *J. Nanosci. Nanotechnol.*, 10 (2010) 1757.
26. Q. Xie, Z. Dai, W. W. Huang, J. B. Liang, C. L. Jiang and Y. T. Qian, *Nanotechnology*, 16 (2005) 2958.
27. Y. R. Ma, L. M. Qi, W. Shen and J. M. Ma, *Langmuir*, 21 (2005) 6161.
28. R. Chen, J. Bi, L. Wu, Z. Li and X. Fu, *Cryst. Growth Des.*, 9 (2015) 1775.
29. B. Gao, H. Q. Fan and X. J. Zhang, *J. Phys. Chem. Solids*, 73 (2012) 423.
30. M. R. Saidur, A. R. A. Aziz and W. J. Basirun, *Bios. Bioelectr.*, 90 (2016) 125.
31. B. Wang, Y. H. Chang and L. J. Zhi, *Carbon*, 26 (2011) 31.
32. V. Jovanovski, S. B. Hočevár and B. Ogorevc, *Electroanalysis*, 21 (2009) 2321.
33. X. Z. Yao, Z. Guo, Q. H. Yuan, Z. G. Liu, J. H. Liu and X. J. Huang, *ACS Appl. Mater. Interfaces*, 6 (2014) 12203.
34. H. H. Zhu, Y. H. Xu, A. Liu, N. Kong, F. K. Shan, W. R. Yang, C. J. Barrow and J. Q. Liu, *Sens. Actuat. B*, 206 (2015) 592.
35. R. O. Kadara and L. E. Tothill, *Anal. Chim. Acta*, 623 (2008) 76.
36. R. X. Xu, X. Y. Yu, C. Gao, Y. J. Jiang, D. D. Han, J. H. Liu and X. J. Huang, *Anal. Chim. Acta*, 790 (2013) 31.
37. R. Devasenathipathy, R. Karthik, S. M. Chen, V. Mani, V. S. Vasantha, M. A. Ali, M. S. Elshikh, B. S. Lou and F. M. A. Al-hemaid, *Electroanalysis*, 27 (2015) 2341.
38. L. Nejd, J. Kudr, B. Ruttkey-Nedecky, Z. Heger, L. Zima, L. Zalud, S. Krizkova, V. Adam, M. Vaculovicova and R. Kizek, *Int. J. Electrochem. Sci.*, 10 (2015) 3635.
39. X. Xuan, M. D. F. Hossain and J. Y. Park, *J. Nanosci. Nanotechnol.*, 16 (2016) 11421.

© 2017 The Authors. Published by ESG (www.electrochemsci.org). This article is an open access article distributed under the terms and conditions of the Creative Commons Attribution license (<http://creativecommons.org/licenses/by/4.0/>).